# Effect of magnetic geometry on the energy partition between ions and electrons in the scrape-off layer of magnetic fusion devices

Y. Li[1,4,5*], G. Xu[4*], B. Dudson[5,8], X. Liu[4], Z. Huang[1], C. Killer[3], Y. Feng[3], S. Liu[4], N. Yan[4], J. Morales[2], E. Tsitrone[2], S. Brezinsek[1], Y. Liang[1], D. Eldon[6], C. Xiao[7], J. Geiger[3], O. Grulke[3], M. Otte[3], the WEST team and the W7-X team

[1]Forschungszentrum Jülich GmbH, Institut für Energie- und Klimaforschung – Plasmaphysik, Partner of the Trilateral Euregio Cluster (TEC), 52425 Jülich, Germany

[2]CEA, IRFM, F-13108 Saint-Paul-lez-Durance, France

[3]Max-Planck-Institut für Plasmaphysik, Greifswald, Germany

[4]Institute of Plasma Physics, Chinese Academy of Sciences, Hefei 230031, China

[5]York Plasma Institute, Department of Physics, University of York, Heslington, York YO10 5DQ, United Kingdom

[6]General Atomics, PO Box 85608, San Diego, CA 92186-5608, USA

[7]Department of Physics and Engineering Physics, University of Saskatchewan, 116 Science Place, Saskatoon, Saskatchewan S7N 5E2, Canada

[8]Lawrence Livermore National Laboratory, 7000 East Ave, Livermore, California 94550

A universal energy partition mechanism between ions and electrons has been confirmed to exist in the scrape-off layer of both the WEST tokamak and the W7-X stellarator. A peaked plasma density structure induced by an infinite magnetic connection length structure is observed to destroy this dependence and enhance the local ion and electron temperature ratio in the stellarator. A theoretical analysis reveals that the ratio of ion and electron parallel heat conduction is predominant in determining this universality, while electrons would further be cooled in the density-peaked region.

## 1. Introduction

Plasma energy partition between ions and electrons is a fundamental topic in the context of astrophysical, geophysical, and magnetically confined fusion plasma, where ions usually maintain much higher temperature than electrons in unconfined or open magnetic field lines, either by preferentially heating from the released magnetic energy during magnetic reconnection[1,2] or due to its less thermal conduction in the region with open magnetic field lines [3]. A key challenge currently encountered in the development of magnetic confined fusion energy is the erosion of the plasma-facing components by ions with energy (~0.1-1keV) across the

last closed magnetic flux surface (LCFS)[4], motivating our efforts to understand the partition of energy between ions and electrons.

To understand the plasma energy partition mechanism, experiments carried out in Tore Supra with limiter configuration [5] and in Alcator C-mod with divertor configuration [6] found that the upstream ion to electron temperature ratio ($\tau_u = T_i/T_e|_u$) approaches unity as the increase of coupling between the ions and electrons, where the term 'upstream' means locations between the field line middle position and divertor entrance. This result is consistent with the two-dimensional fluid simulations for JET and Alcator C-MOD, where $\tau_u$ gradually decreases from ~3 to ~1 as the normalized collisionality ($\nu^*_{SOL,i} = L_\parallel/\lambda_{ii} = 10^{-16} n_u L_\parallel/T^2_{iu}$) gradually increases from ~10 to ~100[3], where $L_\parallel$ is the magnetic connection length from the outboard midplane to divertor target, $\lambda_{ii}$ is the self-collisional mean free path for ions, $n_u$ and $T_{iu}$ are the upstream electron density and ion temperature. However, the current understanding is obtained from limited magnetic connection length regime ($L_\parallel$<100m) and may not be extrapolated to stellarators where the magnetic connection length structure is more complex [7,8]. This paper extends the research scope from tokamaks to the W7-X stellarator where an intrinsic magnetic island topology is formed in the Scrape-off Layer (SOL), significantly enhancing the cross-field transport [9]. We demonstrate experimentally and theoretically, for the first time, that the cross-field transport is negligible comparing with the parallel transport in forming a universal energy partition between ions and electrons when $\beta = (\eta_i + 1)/(\eta_e + 1) > 1$, where $\eta_i = \lambda_{ne}/\lambda_{Ti}$, $\eta_e = \lambda_{ne}/\lambda_{Te}$, $\lambda_{Ti}$, $\lambda_{Te}$ and $\lambda_{ne}$ are the decay lengths of the ion and electron temperature, and plasma density respectively. Nevertheless, a peaked density structure could be induced due to infinite magnetic connection length near the island O point region. This, in turn, destroys the universal dependence and significantly enhances $\tau_u$ by a factor of 3 even in the high collisionality regime. This deviation may worsen wall sputtering on the future W7-X with tungsten divertor and in future stellarator reactors.

## 2. Experimental measurement

Due to the availability of ion temperature measurements by retarding field analyzer (RFA) in the SOL region of both WEST and W7-X [10,11], the upstream plasma parameters including electron temperature and electron density measured by Langmuir probes are studied. Figure 1 shows the magnetic geometries for both devices, where the probes were mounted at the upper side with $R_p$=2553 mm in WEST and at the outer mid-plane at $Z$ = −148 mm and toroidal angle φ=-159.26° in W7-X as indicated with purple bars. Two-dimensional magnetic connection length distributions near the probe paths are also shown in Fig. 1(b-d). WEST is a tokamak with divertor geometry, major radius ~ 2.5 m and effective minor radius ~0.5 m [12].

The magnetic configuration can be changed by adjusting the plasma and external coil currents. The probe measurements are mainly performed for lower single null (LSN) geometry and cover the plasma current $I_p$ ~0.5MA and $q_{95}$~4.5 with some discrete $I_p$ between 0.3 and 0.7 MA, and $q_{95}$ between 3 and 8. W7-X is a quasi-isodynamic stellarator [13] with major radius ~ 5.5 m and effective minor radius ~0.55 m. The intrinsic helical magnetic field could be realized by adjusting the external coil current in the 70 superconducting coils (50 non-planar coils and 20 planar coils). In contrast to the tokamak divertor geometry, there is a chain of magnetic islands in the W7-X plasma boundary to form an intermediate SOL between the confinement core and the plasma-surface interaction region [9]. The so-called standard configuration with $m$=5/$n$=5 islands (edge rotational transform $\iota$=1) is shown in Fig. 1 where the island size was expanded by increasing the additional normal conducting control coil current.

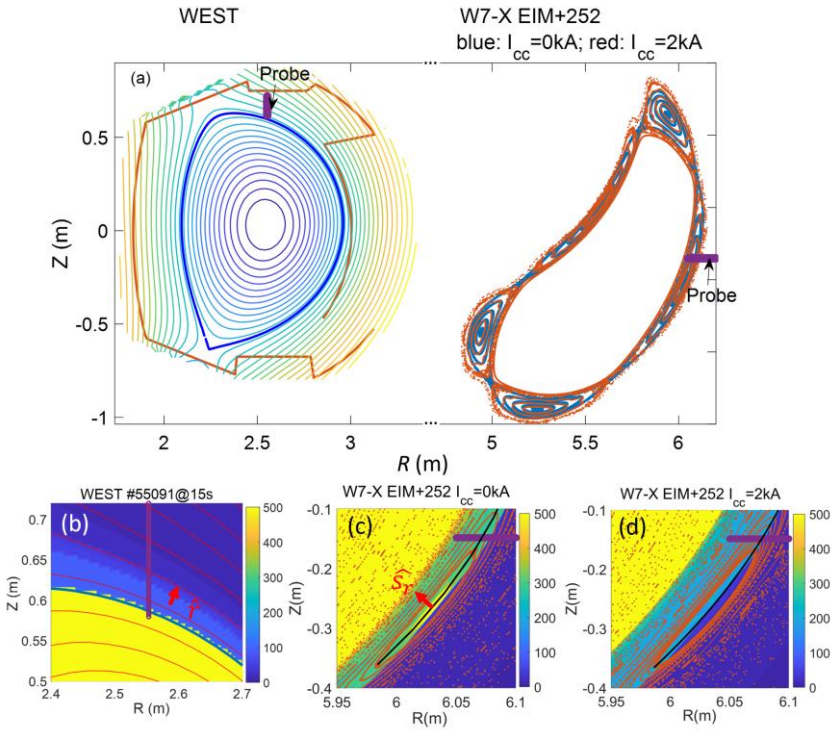


FIG. 1. (a) Magnetic configuration for WEST and W7-X. Connection length distributions superimposed with magnetic configurations are shown in bottom (b) for WEST, (c) $I_{cc}$ =0kA case and (d) $I_{cc}$ =2kA case for W7-X, where the black curve is through the island 'O' and 'X' points, $\hat{r}$ and $\hat{s_r}$ are the unit radial vertors.

The typical profiles of the measured parameter are shown in Fig. 2, where the magnetic connection length between the target points, $L_c = 2L_{\parallel}$, as shown in Fig. 2(e) is calculated by a field line tracing code [14]. The radial profiles have been mapped to the mid-plane for WEST and to the direction normal to the magnetic flux for W7-X. The measured profiles of $T_i$, $T_e$, $n_e$, the derived $\nu^*_{SOL,i}$ and $\tau_u$ in W7-X were strongly affected

by the island geometry [15-17]. Comparing with the measured profiles in WEST, the $T_e$ and $n_e$ profiles in the island geometry form a concave and convex structure respectively near the black curve (named as 'the $\iota$=1 curve') as shown in Fig. 1(c) and (d) which passes O and X points. The $T_i$ profile is still flat near the $\iota$=1 curve and forms a shoulder structure near the steep drop position of the magnetic connection length profile when the control coil current $I_{cc}$ =0kA [15]. When $I_{cc}$ =2kA, the $T_i$ shoulder structure disappears. The derived $\tau_u$ is also significantly enhanced near the $\iota$=1 curve. Expanding the island size would decrease the distance between the island O point and divertor plate, which in turn decreases the magnetic connection length and eliminates the island remnant region near the O point. Consequently, the island effect becomes less important, i.e., the concave and convex degrees and $\tau_u$ near the $\iota$=1 curve become smaller. The effect of the island topology on the plasma was also observed by the He-BES [18] and alkali-BES [19] diagnostics, where a density peak structure can be formed near the island O point.

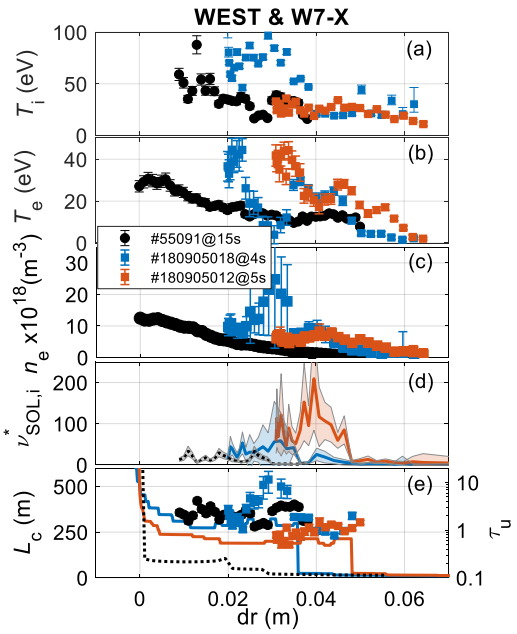


FIG. 2. Profiles of (a) ion and (b) electron temperatures, (c) electron density, (d) normalized ion collisionality and (e) magnetic connection length and $\tau_u$ at the probe paths shown as purple bars in Fig. 1(a). The black dot represents the probe measurement in WEST, and the blue and red squares correspond to the probe measurement in W7-X with control coil current $I_{cc}$ =0kA and $I_{cc}$=2kA, respectively.

A series of ion temperature measurement have been conducted at WEST and W7-X, where the preliminary result for W7-X has been shown in ref. [15]. The plasma heating power includes ohmic, lower hybrid current drive (LHCD) and ion cyclotron resonant frequency (ICRF) for WEST, and only electron cyclotron resonance heating (ECRH) for W7-X. The ranges of the SOL power ($P_{sol}$) and central line

integrated electron density $n_{el}$ are $P_{sol}$ ~[1, 2] MW and $n_{el}$~[3, 5]×$10^{19}$$m^{-2}$ in WEST, and $P_{sol}$~[1, 4] MW and $n_{el}$~[7, 9]x$10^{19}$$m^{-2}$ in W7-X, where the single beam paths within the plasma for the electron density measurement are ~1m in WEST and ~1.33m in W7-X. The working gas is deuterium in WEST and hydrogen in W7-X. $\tau_u$ for both WEST and W7-X at different radial positions as a function of $\nu^*_{SOL,i}$ are shown in Fig. 3, where the sample data, 77 cases for WEST and 10 cases for W7-X, have been averaged over ~1cm radial range for a certain position. For W7-X stellarator, the $\tau_u(\nu^*_{SOL,i})$ dependences for different control coil current cases at the radial position $\Delta r$ =1cm are mixed due to its little effect, while at the radial position $\Delta r$ =0cm are distinguished. For WEST, $\tau_u$ gradually decreases from ~3 to ~1 as $\nu^*_{SOL,i}$ increases from ~5 to ~50, and this tendency exists from the near to far SOL regions. For the W7-X stellarator, $\nu^*_{SOL,i}$ is usually much higher than that in WEST due to longer magnetic connection length. The island geometry was observed to affect the $\tau_u$ tendency. Near the $\iota$=1 curve, i.e., $\Delta r$≈0, $\tau_u$ is significantly enhanced, and this enhancement is reduced by increasing the control coil current. Further away from the $\iota$=1 curve, the $\tau_u$ tendency (blue square in Fig. 3) which has already contained different control coil current cases is close to that in WEST despite the different magnetic topologies in W7-X and WEST.

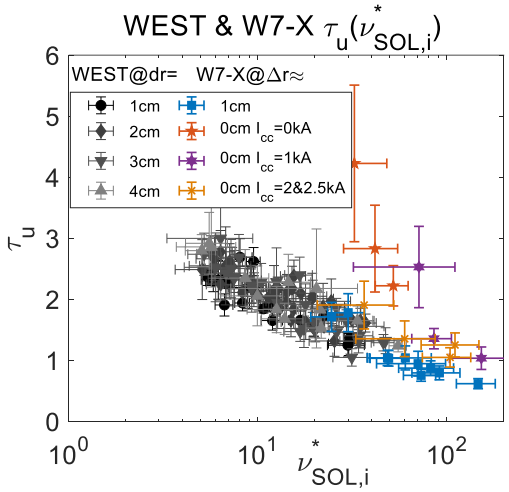


FIG. 3. Ion to electron temperature ratio as a function of normalized ion collisionality for WEST and W7-X at different radial positions. The distance '*dr*' is between the separatrix and the measurement point, and the distance '$\Delta r$' is between the $\iota$=1 curve and the measurement point.

The enhancement of $\tau_u$ at locations near $\Delta r$=0 cm is accompanied by the occurrence of a peaked density structure, at which the electron temperature is cooled while the ion temperature still stays roughly constant. Figure 4 shows $\tau_u$ as functions of $\lambda_{Ti}/\lambda_{Te}$ ratio and $\lambda_{ne}$. The decay lengths of $\lambda_{ne}$, $\lambda_{Te}$ and $\lambda_{Ti}$ for WEST were obtained by exponentially fitting the experimental data which was all selected for Mach number<0.5. For the W7-X stellarator, since the island geometry would strongly affect the parameter profiles,

$\lambda_{ne}$, $\lambda_{Te}$ and $\lambda_{Ti}$ are obtained by calculating the local gradient and average them over roughly 1cm radial range. The island geometry leads to a flatter ion temperature and steeper electron temperature profiles, causing $\lambda_{Ti}/\lambda_{Te}$ ~10, much larger than that in WEST, where $\lambda_{Ti}/\lambda_{Te}$ ~1. The density profile also forms a peaked structure and leads to a local negative $\lambda_{ne}$ near the $\iota$=1 curve. For a certain sign of $\lambda_{ne}$, $\tau_u$ gradually increases with the increase of $1/|\lambda_{ne}|$ for W7-X, while it appears to be independent for WEST. Changing $\lambda_{Ti}/\lambda_{Te}$ for one order of magnitude does not strongly affect $\tau_u$, unless the SOL plasma density gradient is negative, where $\tau_u$ gradually increases with the $\lambda_{Ti}/\lambda_{Te}$ ratio. Note that the $\tau_u$ tendency has also contained different control coil current cases for both $\Delta r_{W7X}$=0 and 1cm positions. The case of $\lambda_{Te} < 0$ near the $\iota$=1 curve is not considered since its location is farther away from the LCFS and close the steep drop position of the $L_C$ profile, where the plasma parameters are affected by the $L_C$ evolution and probe measurement usually behaves larger error.

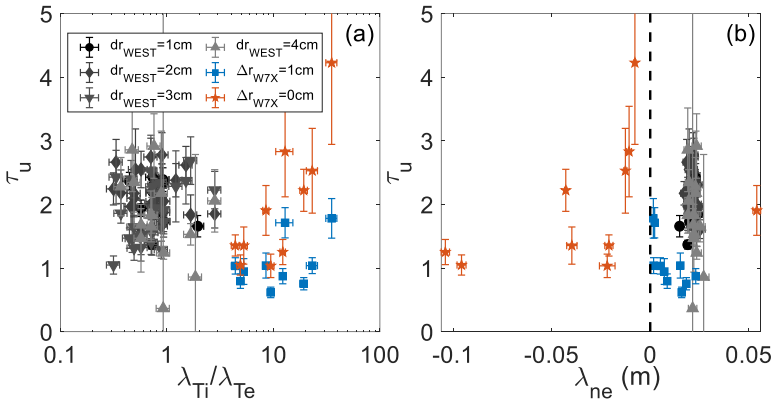


FIG. 4. $\tau_u$ as functions of (a) $\lambda_{Ti}/\lambda_{Te}$ ratio, and (b) $\lambda_{ne}$. The dashed line is used to distinguish the decayed density profile (blue square) and peaked density profile (red star).

### 3. Theoretical analysis

To study the underlying physics, a theoretical analysis is introduced to describe the ion and electron energy transport in the upstream region of SOL for both W7-X and WEST. The idea is based on the ion and electron heat flux transport in the open field line system where the plasma energy would transport first through the LCFS and then be lost in both parallel and perpendicular directions. For simplification, the parallel heat flux loss is balanced with the perpendicular heat flux source plus the energy transfer between ions and electrons. Considering the heat flux flow through a volume, in which no heat source and sink exist, then the thermal energy balance equation satisfies

$$\nabla \cdot \vec{q} = 0 \tag{1}$$

where $\nabla = \nabla_{\parallel} + \nabla_{\perp}$, $\vec{q} = \vec{q}_i + \vec{q}_e$. Considering that ions and electrons exchange their thermal energy inside the volume, Eq. (1) could be split to

$$\nabla \cdot \vec{q}_i = Q_{eq} \tag{2.1}$$

$$\nabla \cdot \vec{q}_e = -Q_{eq} \tag{2.2}$$

where the energy exchange between ions and electrons satisfies $Q_{eq} = \frac{3m_e}{m_i} n_e \nu_{eq}(kT_i - kT_e)$, $\nu_{eq} \approx 2.9 \times 10^{-12} n_e \ln\Lambda T_e^{-3/2}$.

In the SOL upstream region, the parallel heat flux generally satisfies

$$q_{\parallel}^s = q_{\parallel,conv}^s + \left(\frac{1}{q_{\parallel,FL}^s} + \frac{1}{q_{\parallel,SH}^s}\right)^{-1} \tag{3}$$

Where *s* denotes ions (i) or electrons (e) cases. $q_{\parallel,conv}^s$ is the parallel heat convection. $q_{\parallel,FL}^s$ and $q_{\parallel,SH}^s$ are the flux-limited conduction and Spitzer-Härm conduction, respectively. In the experiment, the Mach number has been selected to be smaller than 0.5 for WEST, and smaller than 0.2 for W7-X [15] to minimize the flow effect on the ion temperature measurement. Under this condition, the parallel heat convection is neglected by provided a stationary plasma flow in the upstream region. Since the upstream normalized ion collisionality is selected to be larger than 5, the flux-limited conduction is also neglected [20]. In addition, the nonlocal transport is not considered due to the lack of burst or edge-localized mode (ELM) events in the dataset of WEST and W7-X [21]. Then the parallel heat flux of ions and electrons are simplified to $q_{||}^i = -\kappa_{0i} T_i^{5/2} \frac{\partial T_i}{\partial s_{\parallel}}$, $q_{||}^e = -\kappa_{0e} T_e^{5/2} \frac{\partial T_e}{\partial s_{\parallel}}$, where $s_{\parallel}$ is the parallel step length, $\kappa_{0\mathrm{i}} = \frac{1249}{Z_i^4 m_i^{1/2} \ln\Lambda}$, $\kappa_{0\mathrm{e}} = \frac{30692}{Z_i \ln\Lambda}$, for ion charge $Z_{\mathrm{i}}$=1, mass $m_{\mathrm{i}}$=2, Coulomb logarithm $ln\Lambda = 15$, $\kappa_{0\mathrm{i}} \approx 60$, $\kappa_{0\mathrm{e}} \approx 2000$. Assuming that $\left.\frac{\partial \tau_u}{\partial s_{\parallel}}\right|_u = 0$, then $\left.\frac{\partial T_i}{\partial s_{\parallel}}\right|_u = \tau_u \left.\frac{\partial T_e}{\partial s_{\parallel}}\right|_u$, the ratio of Eq. (2.1) over (2.2) leads to

$$\tau_u^{\frac{7}{2}} = \frac{-Q_{eq} + \nabla_{\perp} \cdot \vec{q}_{\perp}^{\,i}}{Q_{eq} + \nabla_{\perp} \cdot \vec{q}_{\perp}^{\,e}} \frac{K_{0e}}{\mathrm{K_{0i}}} \tag{4}$$

where the perpendicular heat flux of ions and electrons are expressed by $q_{\perp}^i = n\chi_{\perp}^i \nabla_{\perp}(kT_i) + \frac{5}{2} kT_i D_{\perp} \nabla_{\perp} n_e$ and $q_{\perp}^e = n\chi_{\perp}^e \nabla_{\perp}(kT_e) + \frac{5}{2} kT_e D_{\perp} \nabla_{\perp} n_e$, respectively. $D_{\perp}$ and $\chi_{\perp}^{i,e}$ are the perpendicular particle and thermal diffusion coefficient, respectively. The form of differential operator, $\nabla_{\perp}$, depends on the magnetic geometry. For the WEST tokamak, $\nabla_{\perp}$ satisfies $\nabla_{\perp} = \frac{1}{r}\frac{\partial}{\partial r} r$. For the W7-X stellarator, the effective radius of the in-island flux surfaces centered at the O-point, $s_{\mathrm{r}}$, is introduced for the island geometry. The radial coordinate *r* is replaced by $r = r_0 - s_r \approx r_{\mathrm{eff}} - s_r$, where $r_0$ is the distance from the magnetic axis to the

$\iota$=1 curve, and $r_{\mathrm{eff}}$ is the effective minor radius of last closed flux surface. The unit vectors of $\hat{r}$ and $\widehat{s_r}$ are also shown in Fig. 1(b) and (c). Then the differential operator is replaced by $\frac{\partial}{\partial r} = -\frac{\partial}{\partial \mathrm{s_r}}$, i.e., $\nabla_\perp \approx -\frac{1}{r_{\mathrm{eff}}}\frac{\partial}{\partial \mathrm{s_r}} r_{\mathrm{eff}}$.

Assuming that $\frac{\chi_\perp^i}{\lambda_{Ti}} \approx \frac{\chi_\perp^e}{\lambda_{Te}}$, Eq. (4) could be normalized to,

$$\tau_u^{\frac{7}{2}} = \frac{-A_\tau(\tau_u-1)\nu_{SOL,i}^* \tau_u^2 + \tau_u \alpha(\eta_i+1)}{A_\tau(\tau_u-1)\nu_{SOL,i}^* \tau_u^2 + \alpha(\eta_e+1)} \frac{K_{0e}}{\mathrm{K_{0i}}} \tag{5}$$

where $A_\tau = \frac{3}{2}\frac{2}{1.1}\left(\frac{2m_e}{m_i}\right)^{1/2}$, $\alpha = \frac{L_\parallel}{v_{thi,e}\lambda_{ne}}\left(\frac{\chi_\perp^e}{\lambda_{Te}} + \frac{5}{2}\frac{D_\perp}{\lambda_{ne}}\right)$ is a parameter related to the perpendicular transport coefficient, $v_{thi,e} = \sqrt{T_e/m_i}$. The dimensionless parameters $\eta_i$ and $\eta_e$ in the SOL have been measured to be ~1 for limited discharges in Tore Supra [22] and during diverted discharges in JT-60U [23], consistent with the theory prediction that the ITG instability is expected to play a negligible role in driving and regulating SOL turbulence, unless $\eta_i$>2, being the threshold an increasing function of $\tau_u$ and collisionality [24,25]. In W7-X, since $\lambda_{Ti}$ is flattened near the island's O point, $\eta_i$ is generally much smaller than 1, then $\tau_u$ as a function of the two unknown parameters, $\eta_i$ and $\eta_e$, could be simplified to only depend on $(\eta_i+1)/(\eta_e+1)$, i.e., $\beta$. Figure 5 shows $\tau_u$ as functions of $\nu_{SOL,i}^*$ and $\beta$ for different $\alpha$, where $\alpha$ spans over two orders of magnitude. The result shows that $\tau_u$ gradually decreases with the increase of $\nu_{SOL,i}^*$. Increasing the perpendicular transport coefficient, $\alpha$, slightly increases the $\tau_u(\nu_{SOL,i}^*)$ trend when $\beta > 0$, while could significantly enhance $\tau_u$ when $\beta < 0$. The sign of $\beta$ is determined by the plasma density gradient direction. Positive (negative) $\beta$ indicates a decaying (peaked) plasma density profile in the SOL. This result is consistent with the WEST and W7-X measurement where a $\tau_u$ enhancement occurred at the density-peaked locations.

Since increasing $\alpha$ mainly enhances $\tau_u$ for low collsionality value $\nu_{SOL,i}^* \sim 10$ when $\beta > 0$, one could neglect the energy exchange term as $\nu_{SOL,i}^*$ is small and simplify Eq. (5) to

$$\tau_u^{\frac{5}{2}}(\nu_{SOL,i}^*) = \beta \frac{K_{0e}}{\mathrm{K_{0i}}} \tag{6}$$

The right-hand side means the ratio of the ion perpendicular and parallel heat transport over the ratio of the electron perpendicular and parallel heat transport. The $\alpha$ coefficient has been automatically canceled. The term of $\kappa_{0e}/\kappa_{0i} \sim 30$ usually is one order larger than the term of $\beta \sim 1$. This suggests that the classical parallel conductivity is the dominant mechanism governing the $T_i/T_e$ ratio in both the SOL of WEST and W7-X. When the plasma density gradient is reversed, $\beta < 0$, the energy exchange term in Eq. (5) becomes important to balance the energy conservation. In W7-X, since $\lambda_{Ti} \gg \lambda_{Te}$, so $(\eta_e+1)$<0. This implies that

the reversed density gradient accompanies an energy loss from electrons to other particles, such as neutrals, which differs from the ion-electron energy exchange channel. A 2D coherence imaging spectroscopy (CIS) measurements indicate that there is a $C^{2+}$ radiation zone moving from the region close to the divertor target towards LCFS during the transition from the attached to the detached plasma state. Though the electron temperature decreased going into the detachment, the $C^{2+}$ ion temperature was only slightly reduced within the receding $C^{2+}$ layer [26].

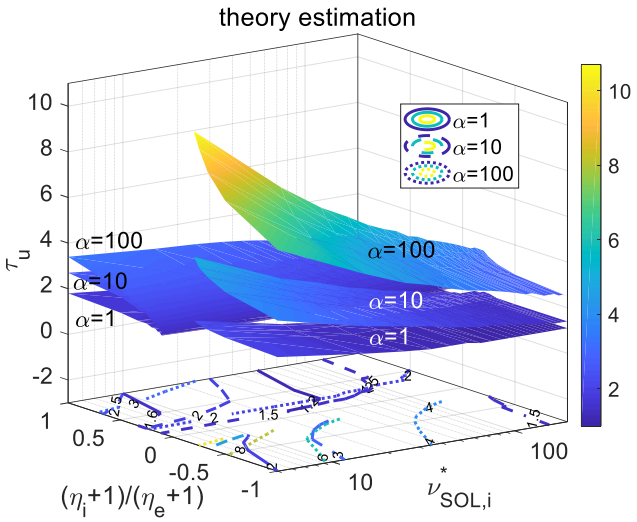


FIG. 5. $\tau_u$ as functions of $\nu^*_{SOL,i}$ and $\beta$ for different α. Note that the contour plot in the bottom displays the isolines of the $\tau_u$ surface to indicate its value variation. Labels in the contour lines represent the $\tau_u$ value. The solid, dashed and dotted lines correspond to α=1, 10 and 100, respectively.

To calculate the perpendicular transport coefficient α, the terms of $\frac{D_\perp}{\lambda_{ne}}$ and $\frac{\chi^e_\perp}{\lambda_{Te}}$ were specified after considering the particle and power conservation equations. For a tokamak divertor geometry, $\frac{D_\perp}{\lambda_{ne}} \approx \frac{\lambda_{ne}}{2}\frac{C_s}{L_\parallel}$ holds [3]. For an island divertor geometry, the magnetic connection length could be infinite near the O point. Based on the particle transport equation, $\frac{d\Gamma_\parallel}{ds_\parallel} = -\frac{d\Gamma_\perp}{ds_\perp} + \mathrm{S_p}$ where $\mathrm{S_p}$ is the ionization source rate, when $L_c \to \infty$, then $\frac{d\Gamma_\parallel}{ds_\parallel} \to 0$ and $\frac{d\Gamma_\perp}{ds_\perp} = S_\mathrm{p}$. This indicates that the ionization source forms density accumulation near the island residual region, i.e., $0<s_r<w_i$, where $w_i$ is the remnant island width. Consequently, there exists a point of minimum density gradient between the separatrix and the island O point, where $\left.\frac{dn}{ds_\perp}\right|_{s_\perp=w_0} = 0$, $w_0$ is the minimum point position. Utilizing the particle balance equation $\frac{d\Gamma_\parallel}{ds_\parallel} = -\frac{d\Gamma_\perp}{ds_\perp}$ in the region $w_i < s_r < w$, where $\Gamma_\parallel = nv_\parallel$ and $\Gamma_\perp = -D_\perp\frac{dn}{ds_\perp}$, one could get $\frac{dn}{ds_\perp} = \frac{1}{D_\perp}\frac{d\Gamma_\parallel}{ds_\parallel}(s_\perp - w_0)$ for the W7-X

stellarator. $\frac{\chi_\perp^e}{\lambda_{Te}}$ could be deduced to be $\frac{\chi_\perp^e}{\lambda_{Te}} \approx A_\chi \lambda_{Te} \frac{T_u^2}{10^{-16} n_u L_\parallel} \frac{v_{thi,e}}{L_\parallel}$ based on the power conservation, *i.e.*, $\frac{dq_\perp}{ds_\perp} \approx -\frac{dq_\parallel}{ds_\parallel}$, where $q_\perp = -K_\perp \frac{dT_e}{ds_\perp}|_u$, $q_\parallel = -K_\parallel \frac{dT_e}{ds_\parallel}|_u$, $K_\perp = e n_e \chi_\perp^e$, $K_\parallel = \kappa_{0e} T_e^{5/2}$, $A_\chi = \frac{4}{49} \frac{10^{-16}}{e} \sqrt{\frac{m_i}{e}} \kappa_{0e}$. Since $\frac{T_u^2}{L n_u} \propto \frac{1}{\nu_{SOL,i}^*}$, $\frac{\chi_\perp^e}{\lambda_{Te}} \approx \frac{A_\chi \lambda_{Te}}{\tau_u^2 \nu_{SOL,i}^*} \frac{v_{thi,e}}{L_\parallel}$, *i.e.*, the term of $\frac{\chi_\perp^e}{\lambda_{Te}}$ gradually decreases with the increase of $\nu_{SOL,i}^*$. Combining the expressions of $\frac{D_\perp}{\lambda_{ne}}$ and $\frac{\chi_\perp^e}{\lambda_{Te}}$, $\alpha$ could be derived to be

$$\alpha \approx \begin{cases} A_\chi \frac{T_u^2}{10^{-16} n_u L_\parallel} \frac{1}{\eta_e} + \frac{5}{4}, \text{WEST} \\ A_\chi \frac{T_u^2}{10^{-16} n_u L_\parallel} \frac{1}{\eta_e} + \frac{5}{4} \frac{s_r - w_0}{\lambda_{ne}}, \text{W7X} \end{cases} \quad (7)$$

Equation (7) indicates that the perpendicular transport coefficient $\alpha$ is independent of the plasma density gradient $\lambda_{ne}$ for WEST tokamak, while gradually increases with the value of $1/|\lambda_{ne}|$. This is consistent with the experimental measurement shown in Fig. 4.

Substituting Eq. (7) into the equivalent form of Eq. (5) as follows, $T_i$ could be estimated based on the measured parameters of $n_e$, $T_e$, $\lambda_{ne}$, $\lambda_{Te}$ and $L_\parallel$.

$$\frac{3m_e}{m_i} \nu_{eq} (T_i - T_e) \left( T_i^{\frac{7}{2}} + T_e^{\frac{7}{2}} \frac{K_{0e}}{K_{0i}} \right) + T_i^{\frac{7}{2}} T_e \alpha \frac{v_{thi,e}}{L_\parallel} (\eta_e + 1) - T_e^{\frac{7}{2}} T_i \alpha \frac{v_{thi,e}}{L_\parallel} (\eta_i + 1) \frac{K_{0e}}{K_{0i}} = 0 \quad (8)$$

The result is shown in Fig. 6, where $\eta_i$ is assumed to be 0.5 for WEST, and 0 for W7-X. Scanning $\eta_i$ would hardly change the $T_i$ estimation. The estimated $T_i$ is generally consistent with the measured $T_i$ in the WEST tokamak for a wide SOL region, and in W7-X for the location with the plasma density decaying from the separatrix. While for the location near the $\iota$=1 curve, the estimated $T_i$ becomes smaller than the measured one. This may be caused by the cooling effect which increases the energy transfer from electrons to neutrals due to ionization and excitation.

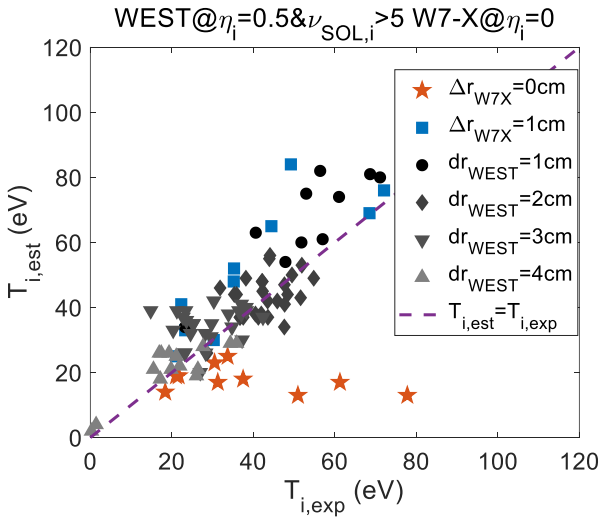


FIG. 6. Estimated upstream ion temperature vs. measured upstream ion temperature on both WEST and W7-

X

## 4. Conclusions

In summary, the effect of magnetic geometry on the energy partition between ions and electrons is studied in the SOL of WEST and W7-X. A universal energy partition mechanism between ions and electrons is confirmed in the upstream region with $\beta > 0$. This universal dependence exists for a wide range of $L_c$ and $\lambda_{Ti}/\lambda_{Te}$. A density-peaked structure induced by the island geometry could destroy this dependence and enhance the local $\tau_u$. This enhancement gradually increases with the increase of $1/|\lambda_{ne}|$ for $\lambda_{ne} < 0$. A theoretical analysis reveals that the ion and electron parallel heat conduction ratio, $\sim K_{0e}/K_{0i}$, is predominant in forming this universal dependence when $\beta > 0$. The perpendicular transport near the island remnant region can lead to plasma density accumulation and significantly enhance $\tau_u$, where the energy sink term from electrons to such as neutrals becomes prominent. Based on this model, an estimated $T_i$ is introduced and is generally consistent with the measured $T_i$ at the SOL of both WEST and W7-X with the normal density gradient direction, while underestimate by a factor of 3 at the peaked plasma density position. This deviation implies that even W7-X and future stellarator reactors are anticipated to operate at high plasma density regime, the island geometry might still induce a high $\tau_u$ in parts of the SOL, where the ion temperature is much higher than the expectations, potentially increasing their metal wall sputtering.

**Acknowledgments**

The authors deeply appreciate the continued research and operational efforts of the entire WEST and W7-X teams. Author Y. Li appreciates J. P. Gunn for the help to get access to the WEST probe data and A. Knieps, P. Drews, A. Nielsen, C. Gil, F. Clairet and D. Vezinet for valuable discussions. This work has been carried out within the framework of the EUROfusion Consortium and has received funding from the Euratom research and training programme 2014-2018 and 2019-2020 under grant agreement No 633053. The views and opinions expressed herein do not necessarily reflect those of the European Commission. The research was also supported by the International Postdoctoral Exchange Fellowship Program under grant 20170009 and the National Natural Science Foundation of China under grant 11705237. This work was in part performed under the auspices of the U.S. DoE by LLNL under Contract DE-AC52-07NA27344.

*Corresponding authors: ylli@ipp.ac.cn and gsxu@ipp.ac.cn

[1] C. P. Wang *et al.*, J. Geophys. Res. **117** A08215 (2012).

[2] M. Hoshino, Astrophys. J. Lett. **868** L18 (2018).

[3] P. C. Stangeby, *The plasma boundary of magnetic fusion devices* (CRC Press, 2000).

[4] G. Federici *et al.*, Nucl. Fusion **41** 1967 (2001).

[5] M. Kocan *et al.*, J. Nucl. Mater. **415** S1133 (2011).

[6] D. Brunner *et al.*, Plasma Phys. Control. Fusion **55** 095010 (2013).

[7] Y. Feng *et al.*, Plasma Phys. Control. Fusion **53** 024009 (2011).

[8] P. Helander *et al.*, Plasma Phys. Control. Fusion **54** 124009 (2012).

[9] Y. Feng *et al.*, Nucl. Fusion **46** 807 (2006).

[10] M. Kočan *et al.*, Rev. Sci. Instrum. **79** 073502 (2008).

[11] M. Henkel *et al.*, Fusion Eng. Des. **157** 111623 (2020).

[12] J. Bucalossi *et al.*, Fusion Eng. Des. **89** 907 (2014).

[13] E. Strumberger, Nucl. Fusion **36** 891 (1996).

[14] S. A. Bozhenkov *et al.*, Fusion Eng. Des. **88** 2997 (2013).

[15] Y. Li *et al.*, Nucl. Fusion **59** 126002 (2019).

[16] C. Killer *et al.*, Nucl. Fusion **59** 086013 (2019).

[17] C. Killer *et al.*, Plasma Phys. Control. Fusion **61** 125014 (2019).

[18] T. Barbui *et al.*, Nucl. Fusion **60** 106014 (2020).

[19] G. Anda *et al.*, Fusion Eng. Des. **146** 1814 (2019).

[20] P. C. Stangeby, J. M. Canik, and D. G. Whyte, Nucl. Fusion **50** 125003 (2010).

[21] J. T. Omotani and B. D. Dudson, Plasma Phys. Control. Fusion **55** 055009 (2013).

[22] M. Kočan and J. P. Gunn, Plasma Phys. Control. Fusion **52** 045010 (2010).

[23] N. Asakura *et al.*, J. Nucl. Mater. **241** 559 (1997).

[24] A. Mosetto *et al.*, Phys. Plasmas **22** 012308 (2015).

[25] J. R. Myra, D. A. D'Ippolito, and D. A. Russell, Phys. Plasmas **22** 042516 (2015).

[26] D. Gradic *et al.*, Nucl. Fusion **61** 106041 (2021).